Supplementary Appendices:
Gaze-Contingent Layered Optical See-Through Displays with a Confidence-Driven View Volume

A Derivation of the Mode Transition Initialization Method

This Section provides a mathematical derivation of Equation 6 in the paper. It is valid if the focal stack contains two images and their respective focus distances correspond to the locations of the display layers. Further, for sake of simplicity, we start by assuming a layered display with an additive image formation process. However during the derivation, we will provide a method to apply it to multiplicative display as well. For a two-layer additive display, we formulate the task of transforming a focal stack to two layer patterns as an optimization problem of the following form [1, 3, 4]:

$$\boldsymbol{p}_i = \underset{\boldsymbol{p}_i,\ i\in\{1,2\}}{\arg\min} \sum_{n=1}^{N=2} ||\hat{\boldsymbol{r}}_n - \sum_{v=1}^{V=2} \boldsymbol{p}_i * c_{v,n}||, \quad \text{s.t. } 0 \leq \boldsymbol{p}_i \leq 1. \tag{1}$$

here p_i refers to the $i-th$ panel, r_n refers to the $n-th$ image of the focal stack, and $c_{v,n}$ refers to the circle-of-confusion on the $v-th, v \in \{1;2\}$ panel when focusing to the $n-th$ image. Using the Simultaneous Algebraic Reconstruction Technique (SART) to solve this problem yields the following iterative update routine:

$$\boldsymbol{p}_i^{(m+1)} = \boldsymbol{p}_i^{(m)} + \frac{1}{VN} \sum_{n=1}^{N=2} w_{i,n} \Big(\hat{\boldsymbol{r}}_n - \sum_{v=1}^{V=2} \boldsymbol{p}_v^{(m)} * c_{v,n} \Big) * c_{n,i} \tag{2}$$

where $w_{i,n}$ refers to the weight given to the $n-th$ focal stack image when updating the $i-th$ panel. Note, the retinal image $\boldsymbol{r}_n$ of the user when focusing to $\hat{\boldsymbol{r}}_n$ (at the m-th iteration) amounts to:

$$\boldsymbol{r}_n^{(m)} = \sum_{v=1}^{V=2} \boldsymbol{p}_v^{(m)} * c_{v,n}. \tag{3}$$

Since the focus distance of the $n-th$ image of the focal stack corresponds to the location of the $i-th$ layer, the circle of confusion $c_{i,n}\big|_{i=n}$ collapses to zero. Hence, for each layer, we can rewrite Equation 3 to:

$$\boldsymbol{r}_i^{(m)}\Big|_{i=n} = \boldsymbol{p}_i^{(m)} + \boldsymbol{p}_j^{(m)} * c_{j,i}, \tag{4}$$

where $j = 1-i$. Further, using the focal image weighting scheme of Ebner et al. [1], which they have shown leads to faster convergence and improved image quality, we apply the weightings: $w_{i,i} = 2, w_{i,j} = 0$. Hence, each layer is updated only with its corresponding image of the focal stack, and Equation 2 becomes:

$$\boldsymbol{p}_i^{(m+1)} = \boldsymbol{p}_i^{(m)} + \frac{1}{2} \Big(\hat{\boldsymbol{r}}_i - (\boldsymbol{p}_i^{(m)} + \boldsymbol{p}_j^{(m)} * c_{i,j}) \Big). \tag{5}$$

Imagine now a display with multiplicative image formation process and the user focusing on panel $\boldsymbol{p}_i$. Each bundle of light that passes through a single pixel in panel $\boldsymbol{p}_i$ passes a range of pixels in panel $\boldsymbol{p}_j$. This range corresponds to the circle of confusion $c_{j,i}$ on the j-th panel when focusing to the i-th panel. Hence, this process can be formulated as:

$$r_i^a = \sum_{c \in \mathcal{C}} L(a,c) = \sum_{c \in \mathcal{C}} (p_i^a \cdot p_j^c), \tag{6}$$

where a light ray $L(a,c)$ landing on an arbitrary pixel a on the retinal image $\boldsymbol{r}_i$, passes through a pixel p_i^a in $\boldsymbol{p}_i$ and a range of pixels in $\boldsymbol{p}_j$ within $\mathcal{C}$. Here, $\mathcal{C}$ is the set of pixels in $\boldsymbol{p}_j$ within an area spanning the circle of confusion $c_{j,i}$.

Taking the log of the light ray yields:

$$log(L(a,c)) = log(p_i^a \cdot p_j^c) = log(p_i^a) + log(p_j^c) = \tilde{p}_i^a + \tilde{p}_j^c. \tag{7}$$

Consequently, the entire log-transformed layer pattern for the $i-th$ layer is referred to as $\tilde{\boldsymbol{p}}_i$. Analogous, we can define the corresponding log-transformed focal stack image, as $\tilde{\boldsymbol{r}}_i$.

Using the log-transformed variables, we can formulate the update rule of Equation 5 for multiplicative layered displays as well:

$$\tilde{\boldsymbol{p}}_i^{(m+1)} = \tilde{\boldsymbol{p}}_i^{(m)} + \frac{1}{2}\left(\tilde{\boldsymbol{r}}_i - (\tilde{\boldsymbol{p}}_i^{(m)} + \tilde{\boldsymbol{p}}_j^{(m)} * c_{i,j})\right), \tag{8}$$

which corresponds to Equation 6 in the main document.

The decomposition approach introduced in the paper consists of the following Equations:

$$\tilde{\boldsymbol{p}}_i^{(m)} = \sum_{k=1}^{\lceil m/2 \rceil} \eta_k \cdot \tilde{\boldsymbol{r}}_i \overset{k-1}{*} \boldsymbol{c}_{j,i} \overset{k-1}{*} \boldsymbol{c}_{i,j} - \sum_{k=1}^{\lfloor m/2 \rfloor} \zeta_k \cdot \tilde{\boldsymbol{r}}_j \overset{k-1}{*} \boldsymbol{c}_{j,i} \overset{k}{*} \boldsymbol{c}_{i,j}, \tag{9}$$

$$\eta_k = \frac{1}{2^m}\left(2^m - \sum_{\mu=0}^{2(k-1)} \binom{m}{\mu}\right), \quad \zeta_k = \frac{1}{2^m}\left(2^m - \sum_{\mu=0}^{2k-1} \binom{m}{\mu}\right), \tag{10}$$

$$\sum_{k=1}^{\lceil m/2 \rceil} (\eta_k - \zeta_k) = 0.5. \tag{11}$$

Prove of Equality The relationship between Equation 9 and 5 can be proven by induction. The first two iterations compute recursively as:

$$\tilde{\boldsymbol{p}}_i^{(1)} = 0.5 \cdot \tilde{\boldsymbol{r}}_i, \tag{12}$$

$$\tilde{\boldsymbol{p}}_i^{(2)} = 0.75 \cdot \tilde{\boldsymbol{r}}_i - 0.25 \cdot \tilde{\boldsymbol{r}}_j * \boldsymbol{c}_{i,j}. \tag{13}$$

Similarly, using Equation 9 and $m = 2$:

$$\tilde{\boldsymbol{p}}_i^{(2)} = \eta_1 \cdot \tilde{\boldsymbol{r}}_i - \zeta_1 \cdot \tilde{\boldsymbol{r}}_j * \boldsymbol{c}_{i,j}. \tag{14}$$

Using Equation 10, we determine that $\eta_1 = 0.5, \zeta_1 = 0.25$, hence Equation 14 and 13 agree. Furthermore, Equation 11 holds. Next, suppose that the equivalence holds for some (even) $m = 2l, l \in \mathbb{N}$. Then, applying Equation 9 to compute $\tilde{\boldsymbol{p}}i^{(m+1)}$ yields

$$\begin{aligned} \tilde{\boldsymbol{p}}_i^{(m+1)} &= \sum_{k=1}^{m/2+1} \eta_k \cdot \tilde{\boldsymbol{r}}_i \overset{k-1}{*} \boldsymbol{c}_{j,i} \overset{k-1}{*} \boldsymbol{c}_{i,j} - \sum_{k=1}^{m/2} \zeta_k \cdot \tilde{\boldsymbol{r}}_j \overset{k-1}{*} \boldsymbol{c}_{j,i} \overset{k}{*} \boldsymbol{c}_{i,j} \\ &= \sum_{k=1}^{m/2} \eta_k \cdot \tilde{\boldsymbol{r}}_i \overset{k-1}{*} \boldsymbol{c}_{j,i} \overset{k-1}{*} \boldsymbol{c}_{i,j} - \sum_{k=1}^{m/2} \zeta_k \cdot \tilde{\boldsymbol{r}}_j \overset{k-1}{*} \boldsymbol{c}_{j,i} \overset{k}{*} \boldsymbol{c}_{i,j} \\ &+ \eta_{m/2+1} \cdot \tilde{\boldsymbol{r}}_i \overset{m/2}{*} \boldsymbol{c}_{j,i} \overset{m/2}{*} \boldsymbol{c}_{i,j}. \end{aligned} \tag{15}$$

On the other hand, if we substitute Equation 5 into Equation 9, we obtain:

$$\begin{aligned}\tilde{\boldsymbol{p}}_i^{(m+1)} =& \frac{1}{2}\left(\tilde{\boldsymbol{p}}_i^{(m)} + \tilde{\boldsymbol{r}}_i - \tilde{\boldsymbol{p}}_j^{(m)} * \boldsymbol{c}_{i,j}\right) \\ =& \frac{1}{2}\left(\sum_{k=1}^{m/2} \eta_{m,k} \cdot \tilde{\boldsymbol{r}}_i \overset{k-1}{*} \boldsymbol{c}_{j,i} \overset{k-1}{*} \boldsymbol{c}_{i,j} - \sum_{k=1}^{m/2} \zeta_{m,k} \cdot \tilde{\boldsymbol{r}}_j \overset{k-1}{*} \boldsymbol{c}_{j,i} \overset{k}{*} \boldsymbol{c}_{i,j}\right) + \frac{\tilde{\boldsymbol{r}}_i}{2} \\ -& \frac{1}{2}\left(\sum_{k=1}^{m/2} \eta_{m,k} \cdot \tilde{\boldsymbol{r}}_j \overset{k-1}{*} \boldsymbol{c}_{i,j} \overset{k-1}{*} \boldsymbol{c}_{j,i} - \sum_{k=1}^{m/2} \zeta_{m,k} \cdot \tilde{\boldsymbol{r}}_i \overset{k-1}{*} \boldsymbol{c}_{i,j} \overset{k}{*} \boldsymbol{c}_{j,i}\right) * \boldsymbol{c}_{i,j}.\end{aligned} \tag{16}$$

In this expression the weights are indexed by m (in addition to k) to distinguish between different decomposition orders. Re-arranging the sums yields

$$\begin{aligned}\tilde{\boldsymbol{p}}_i^{(m+1)} =& \frac{1}{2}\sum_{k=1}^{m/2}\left(\eta_{m,k} \cdot \tilde{\boldsymbol{r}}_i \overset{k-1}{*} \boldsymbol{c}_{j,i} \overset{k-1}{*} \boldsymbol{c}_{i,j} + \zeta_{m,k} \cdot \tilde{\boldsymbol{r}}_i \overset{k}{*} \boldsymbol{c}_{i,j} \overset{k}{*} \boldsymbol{c}_{j,i}\right) + \frac{\tilde{\boldsymbol{r}}_i}{2} \\ -& \frac{1}{2}\sum_{k=1}^{m/2}\left(\eta_{m,k} \cdot \tilde{\boldsymbol{r}}_j \overset{k}{*} \boldsymbol{c}_{i,j} \overset{k-1}{*} \boldsymbol{c}_{j,i} + \zeta_{m,k} \cdot \tilde{\boldsymbol{r}}_j \overset{k-1}{*} \boldsymbol{c}_{j,i} \overset{k}{*} \boldsymbol{c}_{i,j}\right) \\ =& \sum_{k=1}^{m/2-1}\left(\frac{\eta_{m,k} + \zeta_{m,k-1}}{2} \cdot \tilde{\boldsymbol{r}}_i \overset{k}{*} \boldsymbol{c}_{j,i} \overset{k}{*} \boldsymbol{c}_{i,j}\right) + \frac{\eta_{m,1}}{2}\tilde{\boldsymbol{r}}_i + \frac{\zeta_{m,m/2}}{2} \cdot \tilde{\boldsymbol{r}}_i \overset{m/2}{*} \boldsymbol{c}_{i,j} \overset{m/2}{*} \boldsymbol{c}_{j,i} + \frac{\tilde{\boldsymbol{r}}_i}{2} \\ -& \sum_{k=1}^{m/2}\left(\frac{\eta_{m,k} + \zeta_{m,k}}{2} \cdot \tilde{\boldsymbol{r}}_j \overset{k}{*} \boldsymbol{c}_{i,j} \overset{k-1}{*} \boldsymbol{c}_{j,i}\right).\end{aligned} \tag{17}$$

Using this form, it is evident that the coefficients of the convolutions satisfy

$$\eta_{m+1,k} = \frac{\eta_{m,k} + \zeta_{m,k-1}}{2}, \tag{18}$$

$$\zeta_{m+1,k} = \frac{\eta_{m,k} + \zeta_{m,k}}{2}. \tag{19}$$

If we define $\zeta_{m+1,0} = 1$ and $\eta_{m+1,m/2+1} = 0$, the update for $\tilde{\boldsymbol{p}}i^{(m+1)}$ can be written as

$$\begin{aligned}\tilde{\boldsymbol{p}}_i^{(m+1)} =& \sum_{k=1}^{m/2}\left(\eta_{m+1,k} \cdot \tilde{\boldsymbol{r}}_i \overset{k-1}{*} \boldsymbol{c}_{j,i} \overset{k-1}{*} \boldsymbol{c}_{i,j}\right) + \eta_{m+1,m/2+1} \cdot \tilde{\boldsymbol{r}}_i \overset{m/2}{*} \boldsymbol{c}_{i,j} \overset{m/2}{*} \boldsymbol{c}_{j,i} \\ -& \sum_{k=1}^{m/2}\left(\zeta_{m+1,k} \cdot \tilde{\boldsymbol{r}}_j \overset{k}{*} \boldsymbol{c}_{i,j} \overset{k-1}{*} \boldsymbol{c}_{j,i}\right),\end{aligned} \tag{20}$$

which is identical to Equation 15. Thus, the equivalence holds for even m. An analogous argument applies for the case $m = 2l + 1$, with $l \in \mathbb{N}$. Starting from Equation 9, one obtains

$$\begin{aligned}\tilde{\boldsymbol{p}}_i^{(m+1)} =& \sum_{k=1}^{(m+1)/2} \eta_k \cdot \tilde{\boldsymbol{r}}_i \overset{k-1}{*} \boldsymbol{c}_{j,i} \overset{k-1}{*} \boldsymbol{c}_{i,j} - \sum_{k=1}^{(m+1)/2} \zeta_k \cdot \tilde{\boldsymbol{r}}_j \overset{k-1}{*} \boldsymbol{c}_{j,i} \overset{k}{*} \boldsymbol{c}_{i,j} \\ =& \sum_{k=1}^{(m+1)/2} \eta_k \cdot \tilde{\boldsymbol{r}}_i \overset{k-1}{*} \boldsymbol{c}_{j,i} \overset{k-1}{*} \boldsymbol{c}_{i,j} - \sum_{k=1}^{(m-1)/2} \zeta_k \cdot \tilde{\boldsymbol{r}}_j \overset{k-1}{*} \boldsymbol{c}_{j,i} \overset{k}{*} \boldsymbol{c}_{i,j} \\ &+ \zeta_{(m+1)/2} \cdot \tilde{\boldsymbol{r}}_j \overset{(m-1)/2}{*} \boldsymbol{c}_{j,i} \overset{(m+1)/2}{*} \boldsymbol{c}_{i,j}.\end{aligned} \tag{21}$$

Substituting Equation 5 into Equation 9:

$$\begin{aligned}
\tilde{\boldsymbol{p}}_i^{(m+1)} =& \frac{1}{2}\left(\tilde{\boldsymbol{p}}_i^{(m)} + \tilde{\boldsymbol{r}}_i - \tilde{\boldsymbol{p}}_j^{(m)} * \boldsymbol{c}_{i,j}\right) \\
=& \frac{1}{2}\left(\sum_{k=1}^{(m+1)/2} \eta_{m,k} \cdot \tilde{\boldsymbol{r}}_i \overset{k-1}{*} \boldsymbol{c}_{j,i} \overset{k-1}{*} \boldsymbol{c}_{i,j} - \sum_{k=1}^{(m-1)/2} \zeta_{m,k} \cdot \tilde{\boldsymbol{r}}_j \overset{k-1}{*} \boldsymbol{c}_{j,i} \overset{k}{*} \boldsymbol{c}_{i,j}\right) + \frac{\tilde{\boldsymbol{r}}_i}{2} \\
&- \frac{1}{2}\left(\sum_{k=1}^{(m+1)/2} \eta_{m,k} \cdot \tilde{\boldsymbol{r}}_j \overset{k}{*} \boldsymbol{c}_{i,j} \overset{k-1}{*} \boldsymbol{c}_{j,i} - \sum_{k=1}^{(m-1)/2} \zeta_{m,k} \cdot \tilde{\boldsymbol{r}}_i \overset{k}{*} \boldsymbol{c}_{i,j} \overset{k}{*} \boldsymbol{c}_{j,i}\right) \\
=& \sum_{k=1}^{(m-1)/2} \frac{\eta_{m,k} + \zeta_{m,k-1}}{2} \cdot \tilde{\boldsymbol{r}}_j \overset{k-1}{*} \boldsymbol{c}_{j,i} \overset{k-1}{*} \boldsymbol{c}_{i,j} + \frac{\eta_{m,1}}{2} \cdot \tilde{\boldsymbol{r}}_j + \frac{\tilde{\boldsymbol{r}}_i}{2} \\
&- \sum_{k=1}^{(m-1)/2} \frac{\eta_{m,k} + \zeta_{m,k}}{2} \cdot \tilde{\boldsymbol{r}}_j \overset{k-1}{*} \boldsymbol{c}_{j,i} \overset{k}{*} \boldsymbol{c}_{i,j} - \frac{\eta_{m,(m+1)/2}}{2} \cdot \tilde{\boldsymbol{r}}_j \overset{(m-1)/2}{*} \boldsymbol{c}_{j,i} \overset{(m+1)/2}{*} \boldsymbol{c}_{i,j}.
\end{aligned} \tag{22}$$

Using the identities of Equations 18 and 19, this is equivalent to Equation 21. Hence, the Equation also holds for odd m.

Finally, we verify that the recursive relations in Equations 18 and 19 are consistent with the closed-form expression provided in Equation 10. Starting with $\eta_{m+1,k}$ we have

$$\begin{aligned}
\eta_{m+1,k} &= \frac{1}{2^{m+1}}\left(2^m - \sum_{\mu=0}^{2(k-1)} \binom{m}{\mu}\right) + \frac{1}{2^{m+1}}\left(2^m - \sum_{\mu=0}^{2(k-1)-1} \binom{m}{\mu}\right) \\
&= 1 - \frac{1}{2^{m+1}}\left(\sum_{\mu=0}^{2k-2} \binom{m}{\mu} + \sum_{\mu=0}^{2k-3} \binom{m}{\mu}\right).
\end{aligned} \tag{23}$$

Using Pascal's rule

$$\binom{m}{\mu} + \binom{m}{\mu+1} = \binom{m+1}{\mu+1}, \tag{24}$$

we can combine subsequent terms in the two sums (note that $\binom{m}{0} = \binom{m+1}{0} = 1$) to obtain

$$\begin{aligned}
\eta_{m+1,k} &= 1 - \frac{1}{2^{m+1}} \sum_{\mu=0}^{2k-2} \binom{m+1}{\mu} \\
&= \frac{1}{2^{m+1}}\left(2^{m+1} - \sum_{\mu=0}^{2k-2} \binom{m+1}{\mu}\right).
\end{aligned} \tag{25}$$

A similar derivation for $\zeta_{m+1,k}$ leads to

$$\begin{aligned}
\zeta_{m+1,k} &= 1 - \frac{1}{2^{m+1}}\left(\sum_{\mu=0}^{2k-2} \binom{m}{\mu} + \sum_{\mu=0}^{2k-1} \binom{m}{\mu}\right) \\
&= \frac{1}{2^{m+1}}\left(2^{m+1} - \sum_{\mu=0}^{2k-1} \binom{m+1}{\mu}\right).
\end{aligned} \tag{26}$$

Thus, for $m+1$ the expressions in Equations 25 and 26 match the closed-form weights given in Equation 10.

An interesting property of the convolution coefficients $\eta_{m,1}$ and $\zeta_{m,1}$

$$\begin{aligned} \eta_{m,1} &= \frac{2^m - 1}{2^m}, \\ \eta_{m,1} &= \frac{2^m - 1 - m}{2^m}, \end{aligned} \tag{27}$$

is, that the numerator of $\eta_{m,1}$ corresponds to the series of Mersenne numbers (OEIS: A000225), while the numerator of $\zeta_{m,1}$ corresponds to the series of Eulerian numbers (OEIS: A000295).

B Additional Results

B.1 Scenes used for evaluation

The three scenes used throughout the paper for evaluation are depicted in Figure B.1.

Figure B.1: The three scenes used in the evaluation.

B.2 Additional qualitative results

This Section contains qualitative results for scenes a-c with user focus distances of 0.1 dpt, 1 dpt, and 3 dpt. Similar to Figure 9 in the main document, the images contain comparisons between three focus distance offsets ϵ_u for different display types. "Conventional" refers to a single plane display with an image plane at 0.5 dpt, "lf stereoscope" refers to a light field display with static layers presented by Huang et al. [2], a varifocal display, and two of our approaches. "ours worst" represents the unlikely case in which the ground truth focus distance of the user is located significantly outside of the view volume. In "ours best", the focus distance offset ϵ_u corresponds to half of the view volume. SSIM maps for the corresponding images are shown on the botton.

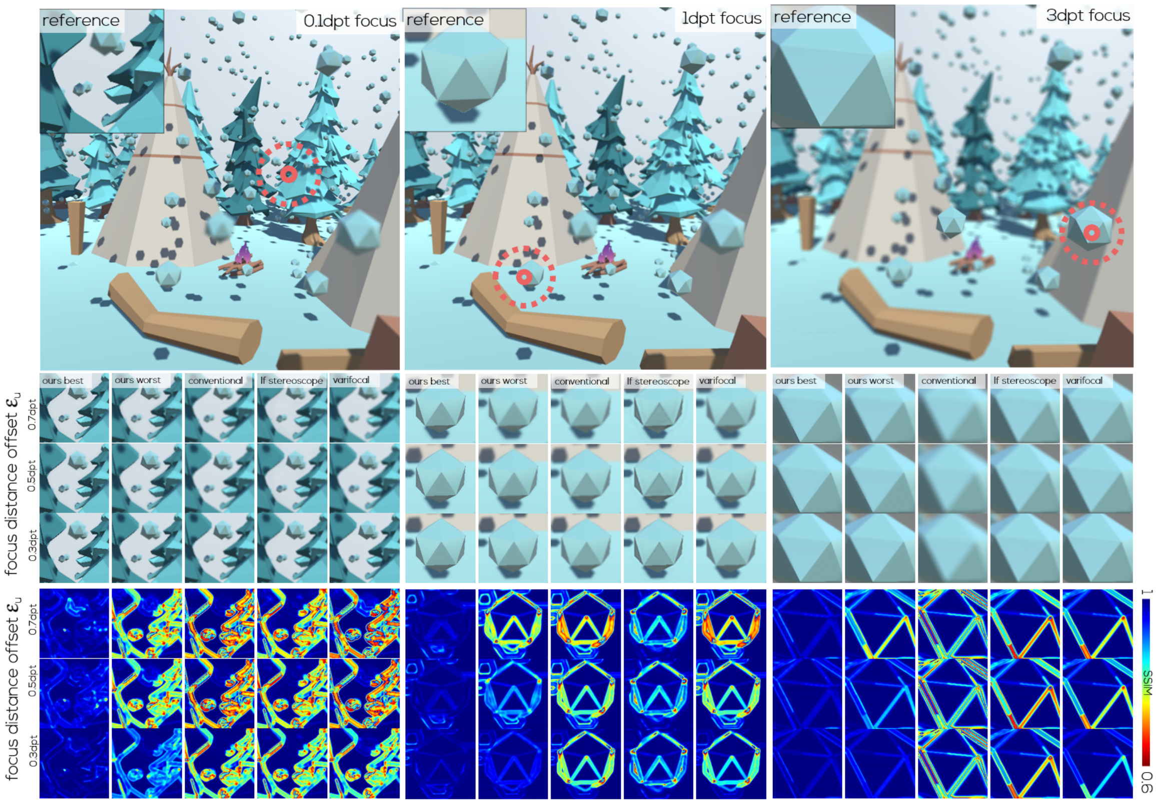

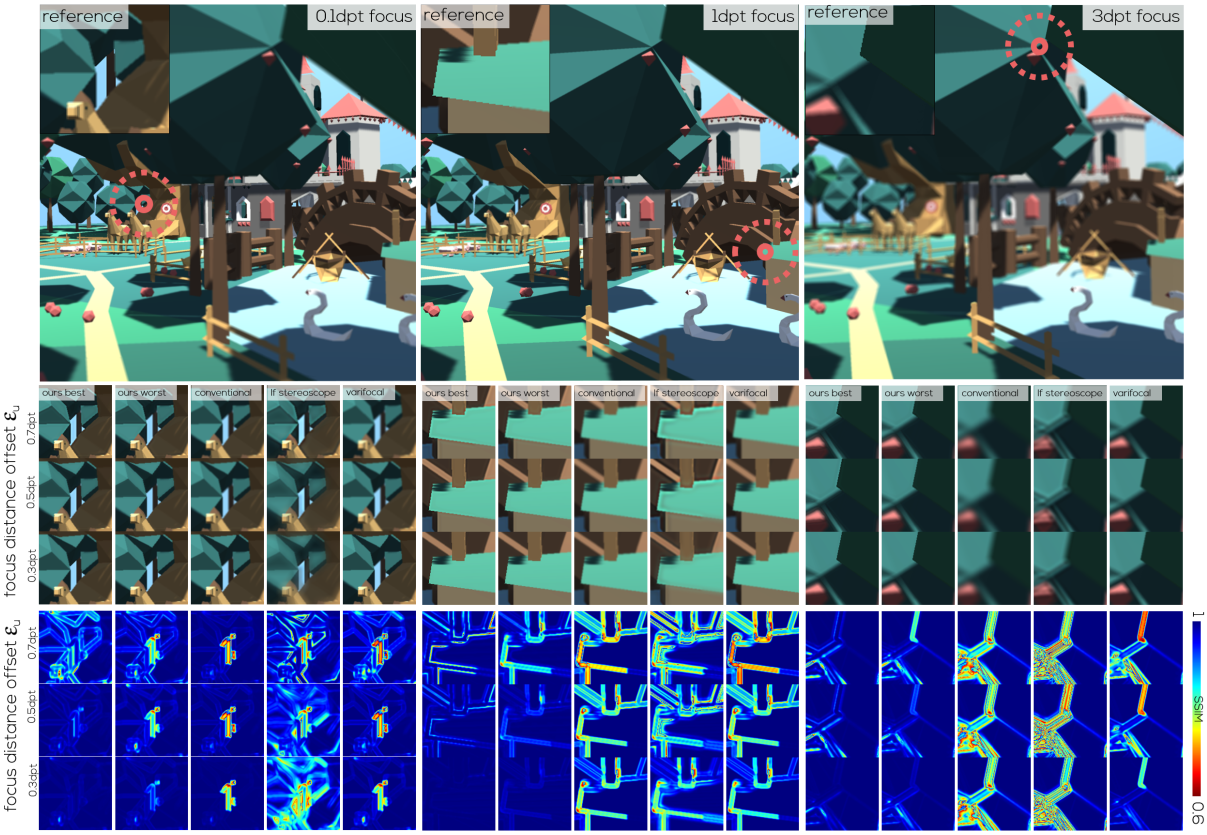
reference
0.1dpt focus
reference
1dpt focus
reference
3dpt focus
ours best
ours worst
conventional
lf stereoscope
varifocal
focus distance offset ϵ_u
0.7dpt
0.5dpt
0.3dpt
SSIM
1
0.6

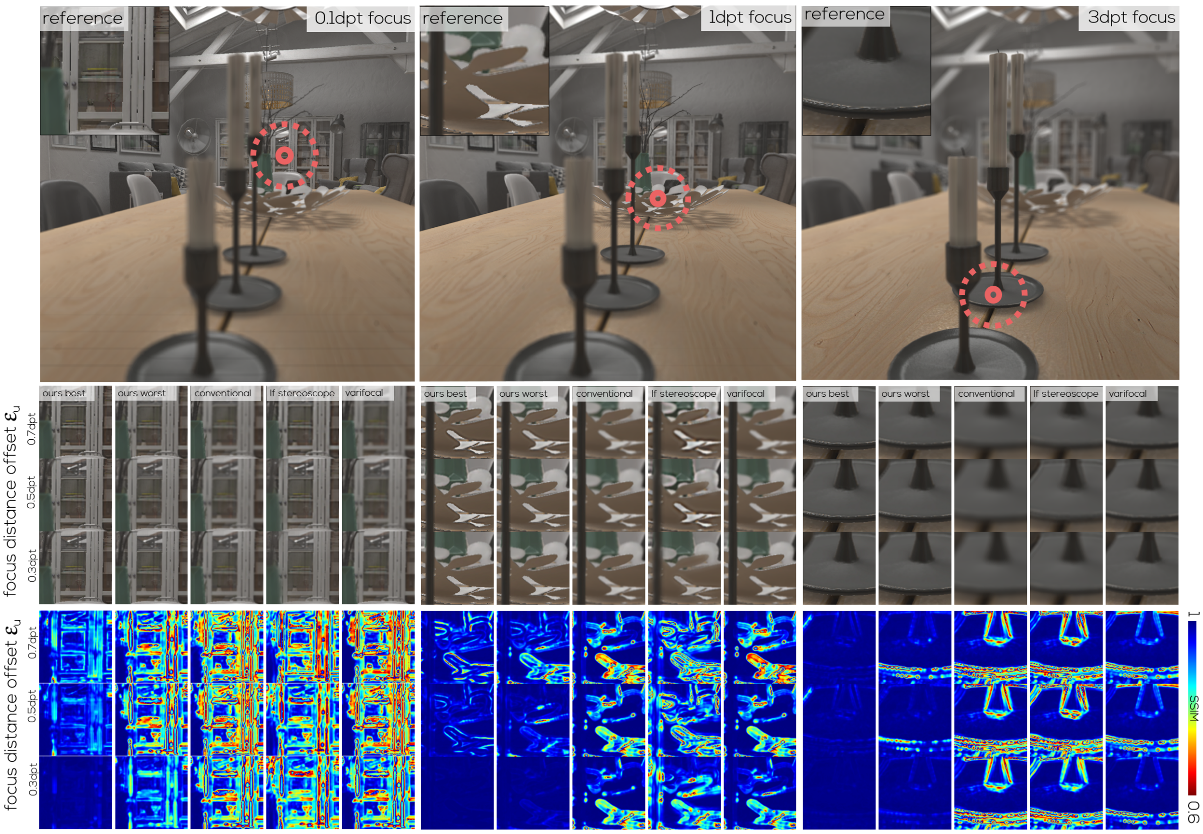
reference
0.1dpt focus
reference
1dpt focus
reference
3dpt focus
ours best
ours worst
conventional
lf stereoscope
varifocal
focus distance offset ϵ_u
0.7dpt
0.5dpt
0.3dpt
SSIM
1
0.6

References

[1] C. Ebner, S. Mori, P. Mohr, Y. Peng, D. Schmalstieg, G. Wetzstein, and D. Kalkofen. Video see-through mixed reality with focus cues. *IEEE Trans. Vis. Comp. Graph.*, 28(5):2256–2266, 2022. doi: 10.1109/TVCG.2022.3150504

[2] F. Huang, K. Chen, and G. Wetzstein. The Light Field Stereoscope: Immersive Computer Graphics via Factored Near-Eye Light Field Displays with Focus Cues. *ACM Transactions on Graphics*, 34(4):1–12, 2015. doi: 10.1145/2766922

[3] S. Lee, J. Cho, B. Lee, Y. Jo, C. Jang, D. Kim, and B. Lee. Foveated retinal optimization for see-through near-eye multi-layer displays. *IEEE Access*, 6:2170–2180, 2017.

[4] H. Yu, M. Bemana, M. Wernikowski, M. Chwesiuk, O. T. Tursun, G. Singh, K. Myszkowski, R. Mantiuk, H.-P. Seidel, and P. Didyk. A perception-driven hybrid decomposition for multi-layer accommodative displays. *IEEE Trans. Vis. Comp. Graph.*, 25(5):1940–1950, 2019.